Numerical implementation of a multiphase model for the analysis and design of reinforced slopes

Ghazi Hassen, Patrick de Buhan

Numerical implementation of a multiphase model for the analysis and design of reinforced slopes

Ghazi Hassen, Patrick de Buhan
LMSGC (LCPC, ENPC, CNRS, UMR 113), Ecole Nationale des Ponts et Chaussées, France
E-mail: hassen@lmsgc.enpc.fr

Abstract. A multiphase model is proposed for the elastoplastic analysis and design of soil structures reinforced by stiff linear inclusions, where shear and bending effects should be taken into account. A f.e.m-based numerical tool, incorporating a plasticity algorithm adapted to this multiphase model, is developed and illustrated on the example of a slope stabilized by such reinforcing inclusions. Emphasis is put in this analysis on the crucial role played by the shear and flexural behaviour of the inclusions in the slope stabilization.

Keywords: reinforced soil; multiphase model; elastoplastic behaviour; shear and bending effects; slope stability.

1 INTRODUCTION

The use of reinforcing inclusions in order to enhance the stability or improve the performance of geotechnical structures, has been widely developed for several decades in the field of geotechnical engineering. The so-obtained composite soil structure exhibits a strong heterogeneity, which leads to intractable, or at least computational time-consuming difficulties, when trying to simulate the response of this kind of structure numerically, by means for instance of finite element techniques. As an alternative approach, a so-called multiphase model of reinforced soil structures has been recently proposed (de Buhan and Sudret, 2000), in which the soil mass and reinforcement network are treated as mutually interacting superposed homogeneous continua. The numerical implementation of such a multiphase model leads to a considerably shorter computational time than the use of a direct simulation. As regards some applications, such as reinforced earth or even soil nailing, in which "flexible" inclusions are used, a simplified version of this multiphase model, where only axial forces in the reinforcements are taken into account, remains sufficient. On the contrary, in the case of a reinforcement by "rigid" inclusions, such as piled raft foundations or pile reinforced slopes, a more elaborate version of this model should be proposed, where shear and bending effects are accounted for, through an idealization of the inclusions as 1D-beams continuously distributed throughout the matrix

The present contribution is devoted to the extension of the latter model to the context of elastoplasticity, the behavior of each phase being characterized by its elastic and plastic properties. As concerns the reinforcement phase, it appears that the elastic parameters to be introduced in the model may be interpreted as the axial, shear and bending stiffnesses of the reinforcements, per unit transverse area, while the yield criterion is formulated as a condition involving both the axial force and bending moment densities. A variational formulation and related finite element implementation of the model has been performed in the particular case when a perfect bonding condition between matrix and reinforcement phases may be assumed. Restricting for instance the analysis to plane strain problems, three independent kinematic variables (two displacements and one rotation) are attached to each node of the finite element mesh (Hassen and de Buhan, 2005*a*). The elastoplasticity is then treated for each phase separately by means of the classical iterative procedure which combines an elastic calculation with prescribed non elastic strains defined in both phases and a local projection of the trial states of stress in each phase on the corresponding yield strength domain. A finite element computational tool dedicated to the analysis of two-dimensional (plane strain) problems has been developed and used to simulate the behavior of a slope under weight loading.

2 TWO-PHASE MODEL OF REINFORCED SOILS

Consider any volume of homogeneous soil reinforced by a network of regularly distributed linear inclusions oriented along the same direction *Ox*. According to the two-phase model (de Buhan and Sudret, 2000), the composite reinforced soil is regarded as the superposition of two continuous media, called matrix and reinforcement phases, respectively. This notably means that matrix and reinforcement particles are geometrically coincident at any point, but may be attributed different kinematics.

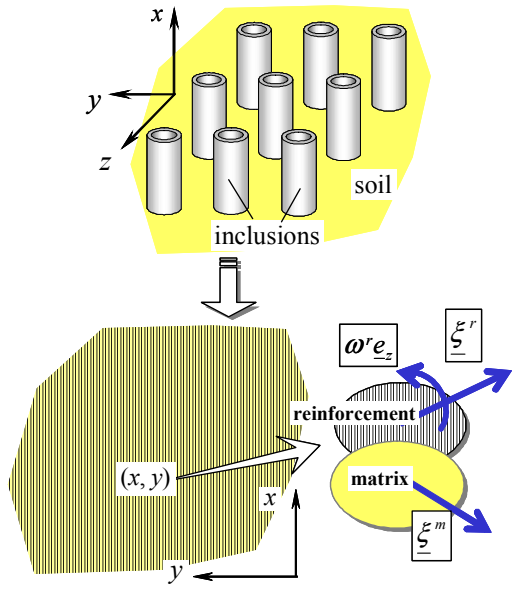

Figure 1 Plane strain kinematics of a two-phase model of reinforced soil

Restricting our analysis to plane strain problems, the matrix phase (which represents the soil) is endowed with the kinematics of a classical Cauchy continuum, characterised at any point by a displacement vector $\underline{\xi}^m$, whereas the reinforcement phase (inclusions) is modelled as a micropolar continuum (Cosserat medium), the kinematics of which is defined in each point by a displacement vector $\underline{\xi}^r$, along with a rotation $\omega^r \underline{e}_z$ (Figure 1).

3 STATICS OF THE MODEL

Starting from this kinematic description, the virtual work method, and related principles, allows to obtain the set of equations governing the equilibrium of such a multiphase continuum (see Sudret, 1999) for more details). Those equations may be written as follows, for each phase separately:

$$\mathrm{div}\underline{\underline{\sigma}}^m + \rho^m \underline{F}^m + \underline{I} = 0 \tag{1}$$

for the matrix phase, and:

$$\begin{aligned} &\mathrm{div}(n^r \underline{e}_x \otimes \underline{e}_x + v^r \underline{e}_y \otimes \underline{e}_x) + \rho^r \underline{F}^r - \underline{I} = 0 \\ &\mathrm{div}(m^r \underline{e}_z \otimes \underline{e}_x) + v^r \underline{e}_z = 0 \end{aligned} \tag{2}$$

for the reinforcement phase, where:

◊ $\underline{\underline{\sigma}}^m$ is the Cauchy stress tensor defined in each point of the matrix phase;

◊ n^r, v^r and m^r denote the densities of axial and shear forces, and bending moment, per unit transverse area to the reinforcement orientation;

◊ $\rho^m \underline{F}^m$ (resp. $\rho^r \underline{F}^r$) is the volume density of external body forces applied to the matrix phase (resp. reinforcement phase);

◊ $\underline{I}$ is the matrix-reinforcement interaction force volume density.

Stress boundary conditions are also prescribed for each phase separately.

4 ELASTOPLASTIC CONSTITUTIVE BEHAVIOUR

In the context of small perturbations, the deformations in the matrix phase are classically described by the linearized strain tensor $\underline{\underline{\varepsilon}}^m$, while as regards the reinforcement phase, three strain variables, analogous to those encountered in the classical beam theory, are introduced, namely the axial strain ε^r, shear strain θ^r and curvature χ^r, defined as:

$$\varepsilon^r = \frac{\partial \xi_x^r}{\partial x} \;,\quad \theta^r = \frac{\partial \xi_y^r}{\partial x} - \omega^r \;,\quad \chi^r = \frac{\partial \omega^r}{\partial x} \tag{3}$$

Besides, the matrix-reinforcement interaction strain variable is:

$$\Delta\underline{\xi} = \underline{\xi}^m - \underline{\xi}^r \tag{4}$$

For the matrix phase the elastoplastic behaviour could be expressed by the constitutive law:

$$\underline{\underline{\sigma}}^m = \lambda^m \,\mathrm{tr}\left(\underline{\underline{\varepsilon}}^m - \underline{\underline{\varepsilon}}^m_{\mathrm{p}}\right)\underline{\underline{1}} + 2\mu^m \left(\underline{\underline{\varepsilon}}^m - \underline{\underline{\varepsilon}}^m_{\mathrm{p}}\right) \tag{5}$$

where λ^m and μ^m are the Lamé coefficients and $\underline{\underline{\varepsilon}}^m_{\mathrm{p}}$ is the plastic strain tensor, the evolution of which is governed by a plastic flow rule:

$$\dot{\underline{\underline{\varepsilon}}}^m_{\mathrm{p}} = \dot{\eta}^m \frac{\partial g^m}{\partial \underline{\underline{\sigma}}^m} \;\text{ with }\; \dot{\eta}^m = \begin{cases} \geq 0 \text{ if } f(\underline{\underline{\sigma}}^m) = \dot{f}(\underline{\underline{\sigma}}^m) = 0 \\ = 0 \text{ otherwise} \end{cases} \tag{6}$$

where f^m is the yield function and g^m the plastic yield potential, these two functions being coincident in the case of an associated flow rule.

As concerns the reinforcement phase, the elastoplastic constitutive behaviour may be expressed in the form of three stress-strain scalar relationships

$$n^r = \alpha^r(\varepsilon^r - \varepsilon^r_{\mathrm{p}}) \;,\; v^r = \beta^r(\theta^r - \theta^r_{\mathrm{p}}) \;,\; m^r = \gamma^r(\chi^r - \chi^r_{\mathrm{p}}) \tag{7}$$

where α^r, β^r and γ^r are the axial, shear and flexural stiffness densities of the reinforcements, per unit transverse area to the reinforcement orientation. The yield function, which defines the elastic domain, is formulated as a function of the three generalised stress components:

$$f^r(n^r, v^r, m^r) \leq 0 \tag{8}$$

and the evolution of the plastic parts of the reinforcement-phase strain variables are expressed through the plastic flow rule:

$$\dot{\varepsilon}^r_{\mathrm{p}} = \dot{\eta}^r \frac{\partial f^r}{\partial n^r} \;,\; \dot{\theta}^r_{\mathrm{p}} = \dot{\eta}^r \frac{\partial f^r}{\partial v^r} \;,\; \dot{\chi}^r_{\mathrm{p}} = \dot{\eta}^r \frac{\partial f^r}{\partial m^r} \tag{9}$$

Likewise, the matrix-reinforcement interaction constitutive behaviour may be expressed as:

$$\underline{I}=\underline{\underline{c}}^{I}\left[\Delta\underline{\xi}-\Delta\underline{\xi}_{\mathrm{p}}\right] \tag{10}$$

where $\underline{\underline{c}}^{I}$ is the interaction stiffness tensor and:

$$\Delta\underline{\xi}_{\mathrm{p}}=\dot{\eta}^{I}\frac{\partial g^{I}}{\partial\underline{I}} \text{ with } \dot{\eta}^{I}=\begin{cases}\geq 0 \text{ if } f^{I}(\underline{I})=\dot{f}^{I}(\underline{I})=0\\ =0 \text{ otherwise}\end{cases} \tag{11}$$

where , f^{I} (resp. g^{I}) is the yield criterion (resp. potential).

5 NUMERICAL IMPLEMENTATION

A finite element formulation of the model has been developed, first in the context of elasticity, then extended to take into account the elastoplastic behaviour of the different constituents (matrix and reinforcement phases), whereas perfect bonding is assumed between the reinforcement and matrix phases.

Denoting by $\{Q\}$ the set of loading parameters to which the structure is subjected, any loading path may be divided into sufficiently small load increments $\{\Delta Q\}$ defined as:

$$\{\Delta Q\}=\{Q\}(t+\Delta t)-\{Q\}(t) \tag{12}$$

Assuming now that the solution has been determined up to the load value $\{Q\}(t)$, in terms of displacement-rotation fields $\{\xi,\omega^{r}\}(t)$, generalized stress fields $\{\underline{\underline{\sigma}}^{m}, (n^{r},v^{r},m^{r})\}(t)$, and plastic strain fields $\{\underline{\underline{\varepsilon}}^{m}{}_{\mathrm{p}},(\varepsilon^{r}{}_{\mathrm{p}}, \theta^{r}{}_{\mathrm{p}}, \chi^{r}{}_{\mathrm{p}})\}(t)$, the problem consists in updating the solution at time $t+\Delta t$ associated with the application of the load increment $\{\Delta Q\}$. This solution may be obtained by adding to the solution at time t, the solution of an *elastic problem* relative to the application of the load increment $\{\Delta Q\}$, the *plastic strain increments* $\{\Delta\underline{\underline{\varepsilon}}^{m}{}_{\mathrm{p}},(\Delta\varepsilon^{r}{}_{\mathrm{p}}, \Delta\theta^{r}{}_{\mathrm{p}}, \Delta\chi^{r}{}_{\mathrm{p}})\}$ being prescribed as non-elastic strains. This may be written as:

$$\begin{aligned}&\begin{Bmatrix}\Delta\underline{\underline{\sigma}}^{m};(\Delta n^{r},\Delta v^{r},\Delta m^{r})\\ \Delta\underline{\underline{\varepsilon}}^{m};(\Delta\varepsilon^{r},\Delta\theta^{r},\Delta\chi^{r})\end{Bmatrix}\\ &=\mathrm{Elas.}\left[\{\Delta Q\},\left\{\Delta\underline{\underline{\varepsilon}}^{m}_{\mathrm{p}};(\Delta\varepsilon^{r}_{\mathrm{p}},\Delta\theta^{r}_{\mathrm{p}},\Delta\chi^{r}_{\mathrm{p}})\right\}\right]\end{aligned} \tag{13}$$

Those plastic strain increments must themselves satisfy the plastic flow rules (6) and (9), expressed in their incremental form as:

$$\Delta\underline{\underline{\varepsilon}}^{m}_{\mathrm{p}}=\Delta\eta^{m}\frac{\partial f^{m}}{\partial\underline{\underline{\sigma}}^{m}}(\underline{\underline{\sigma}}^{m}+\Delta\underline{\underline{\sigma}}^{m}) \ , \ \Delta\eta^{m}\geq 0 \tag{14}$$

for the matrix phase, and

$$\begin{cases}\Delta\varepsilon^{r}_{\mathrm{p}}=\Delta\eta^{r}\dfrac{\partial f^{r}}{\partial n^{r}}(n^{r}+\Delta n^{r})\\ \Delta\theta^{r}_{\mathrm{p}}=\Delta\eta^{r}\dfrac{\partial f^{r}}{\partial v^{r}}(v^{r}+\Delta v^{r}) \quad , \quad \Delta\eta^{r}\geq 0\\ \Delta\chi^{r}_{\mathrm{p}}=\Delta\eta^{r}\dfrac{\partial f^{r}}{\partial m^{r}}(m^{r}+\Delta m^{r})\end{cases} \tag{15}$$

for the reinforcement phase.

Combining these relationships with the constitutive equations (5) and (7) also expressed in their incremental form, finally yields:

$$\underline{\underline{\sigma}}^{m}+\Delta\underline{\underline{\sigma}}^{m}=\underset{\mathrm{C}^{m}}{\mathrm{proj.}}\left\{\underline{\underline{\sigma}}^{m}+\underline{\underline{\underline{\underline{C}}}}^{m}:\Delta\underline{\underline{\varepsilon}}^{m}\right\} \tag{16}$$

and:

$$\begin{aligned}&(n^{r}+\Delta n^{r},v^{r}+\Delta v^{r},m^{r}+\Delta m^{r})=\\ &\underset{\mathrm{C}^{r}}{\mathrm{proj.}}\left\{n^{r}+\alpha^{r}\Delta\varepsilon^{r},v^{r}+\beta^{r}\Delta\theta^{r},m^{r}+\gamma^{r}\Delta\chi^{r}\right\}\end{aligned} \tag{17}$$

where proj.{.} denotes the *projection* onto the convex elastic domains C^{m} or C^{r}, defined by the matrix (resp. reinforcement) phase yield condition, these projections being calculated in the sense of the scalar products defined by:

$$\left\langle\underline{\underline{\sigma}},\underline{\underline{\sigma}}'\right\rangle=1/2\,\underline{\underline{\sigma}}:(\underline{\underline{\underline{\underline{C}}}}^{m})^{-1}:\underline{\underline{\sigma}}' \ , \ \underline{\underline{\underline{\underline{C}}}}^{m}:\text{elastic stiffness tensor} \tag{18}$$

for the matrix phase stresses, and:

$$\left\langle(n,v,m),(n',v',m')\right\rangle=1/2\left(\frac{nn'}{\alpha^{r}}+\frac{vv'}{\beta^{r}}+\frac{mm'}{\gamma^{r}}\right) \tag{19}$$

for the reinforcement stress variables.

This system of equations is classically solved by means of an iterative procedure, called *return mapping algorithm* (Crisfield, 1991; Simo and Hughes, 1998). Starting the iterative procedure from i=0, where all the plastic strain increments are taken equal to zero, and assuming that their values have been calculated up to iteration n°i, these values are updated at the next iteration i+1 through the following steps:

(i) Calculate the corresponding elastic solution incorporating these plastic strain increments as prescribed non-elastic strains:

$$\begin{aligned}&\begin{Bmatrix}\Delta\underline{\underline{\sigma}}^{m};(\Delta n^{r},\Delta v^{r},\Delta m^{r})\\ \Delta\underline{\underline{\varepsilon}}^{m};(\Delta\varepsilon^{r},\Delta\theta^{r},\Delta\chi^{r})\end{Bmatrix}(i)\\ &=\mathrm{Elas.}\left[\{\Delta Q\},\left\{\Delta\underline{\underline{\varepsilon}}^{m}_{\mathrm{p}};(\Delta\varepsilon^{r}_{\mathrm{p}},\Delta\theta^{r}_{\mathrm{p}},\Delta\chi^{r}_{\mathrm{p}})\right\}(i)\right]\end{aligned} \tag{20}$$

(ii) Determine the projections of the different trial stress states onto the respective elastic domains:

$$\underline{\underline{\sigma}}^{m}_{\mathrm{p.a.}}(i)=\underset{\mathrm{C}^{m}}{\mathrm{proj.}}\left\{\underline{\underline{\sigma}}^{m}+\underline{\underline{\underline{\underline{C}}}}^{m}:\Delta\underline{\underline{\varepsilon}}^{m}(i)\right\} \tag{21}$$

$$\begin{aligned}&(n^{r}_{\mathrm{p.a.}},v^{r}_{\mathrm{p.a.}},m^{r}_{\mathrm{p.a.}})(i)=\\ &\underset{\mathrm{C}^{r}}{\mathrm{proj.}}\left\{n^{r}+\alpha^{r}\Delta\varepsilon^{r}(i),v^{r}+\beta^{r}\Delta\theta^{r}(i),m^{r}+\gamma^{r}\Delta\chi^{r}(i)\right\}\end{aligned} \tag{22}$$

(iii) Compute the updated plastic strain increments at iteration i+1 as:

$$\begin{aligned}\Delta\underline{\underline{\varepsilon}}^{m}_{\mathrm{p}}(i+1)&=\Delta\underline{\underline{\varepsilon}}^{m}(i)+(\underline{\underline{\underline{\underline{C}}}}^{m})^{-1}:\left(\underline{\underline{\sigma}}^{m}-\underline{\underline{\sigma}}^{m}_{\mathrm{p.a.}}(i)\right)\\ &=\Delta\underline{\underline{\varepsilon}}^{m}_{\mathrm{p}}(i)+(\underline{\underline{\underline{\underline{C}}}}^{m})^{-1}:\left(\underline{\underline{\sigma}}^{m}+\Delta\underline{\underline{\sigma}}^{m}(i)-\underline{\underline{\sigma}}^{m}_{\mathrm{p.a.}}(i)\right)\end{aligned} \tag{23}$$

and

$$\begin{cases} \Delta\varepsilon_{\mathrm{p}}^{r}(i+1)=\Delta\varepsilon^{r}(i)+\dfrac{1}{\alpha^{r}}\left(n^{r}-n_{\mathrm{p.a.}}^{r}(i)\right) \\ \Delta\theta_{\mathrm{p}}^{r}(i+1)=\Delta\theta^{r}(i)+\dfrac{1}{\beta^{r}}\left(v^{r}-v_{\mathrm{p.a.}}^{r}(i)\right) \\ \Delta\chi_{\mathrm{p}}^{r}(i+1)=\Delta\chi^{r}(i)+\dfrac{1}{\gamma^{r}}\left(m^{r}-m_{\mathrm{p.a.}}^{r}(i)\right) \end{cases} \tag{24}$$

This iterative procedure is carried out until convergence, which corresponds for instance to the fact that the sequences of P.A. and S.A. stress fields tend simultaneously towards the solution:

$$\begin{aligned} &\lim_{i\to\infty}\left\{\underline{\underline{\sigma}}_{\mathrm{p.a.}}^{m};(n_{\mathrm{p.a.}}^{r},v_{\mathrm{p.a.}}^{r},m_{\mathrm{p.a.}}^{r})\right\}(i) \\ &=\left\{\underline{\underline{\sigma}}^{m}+\Delta\underline{\underline{\sigma}}^{m};(n^{r}+\Delta n^{r},v^{r}+\Delta v^{r},m^{r}+\Delta m^{r})\right\} \end{aligned} \tag{25}$$

It should be noted that, while steps (*ii*) and (*iii*) are associated with the *local* treatment of plasticity, which is carried out for each phase independently, step (*i*) corresponds to a *global* elastic calculation.

6 APPLICATION TO THE DESIGN OF A REINFORCED SLOPE

A finite element code based upon the above described numerical implementation of the two-phase model, has been set up and validated on theoretical solutions dealing with two-phase structures. A first application of this numerical tool is the design of piled raft foundations subjected to combined loadings, showing in particular that the flexural stiffness and strength properties of the inclusions play an important role to ensure the stability of such structures subject to both lateral loading and overturning moment (Hassen and de Buhan, 2005*a* and *b*).

The numerical tool is applied here to analyse the stability of a slope of angle β (Figure 2) subject to its own weight, made of a superficial layer of soft soil of thickness D lying upon a soil having better mechanical characteristics. Both soils are purely cohesive materials (clays) of elastoplastic characteristics (E_1, ν_1, C_1) for the upper one and (E_2, ν_2, C_2) for the lower one. Their specific weights are denoted by γ_1 and γ_2, repectively. The following geometrical characteristics have been selected:

$$\tan\beta=1/2, D=13\mathrm{m}, H=10\mathrm{m}, L=70\mathrm{m}, B=40\mathrm{m}, B'=50\mathrm{m} \tag{26}$$

The upper surface layer is given the following mechanical characteristics:

$$E_1=5\,\mathrm{MPa}, \nu_1=0.3, C_1=10\mathrm{kPa}, \gamma_1=18\mathrm{kN/m^3} \tag{27}$$

while the underlying soil displays much stronger characteristics:

$$E_2=100\mathrm{MPa}, \nu_2=0.3, C_2=100\mathrm{kPa}, \gamma_2=25\mathrm{kN/m^3} \tag{28}$$

As shown in figure 2, this slope has been reinforced in its central part by a group of vertical tubular piles of radius R=1m, thickness t=0.02m and length equal to the superficial soft layer. The reinforcing inclusions are placed into the soil mass following a regular square mesh of s=5m side. There are made of a steel having the following characteristics:

$$E^{s}=200\,\mathrm{GPa}, \nu^{s}=0.3, \sigma_{\mathrm{Y}}^{s}=200\,\mathrm{MPa} \tag{29}$$

where σ_{Y}^{s} is the steel uniaxial yield strength.

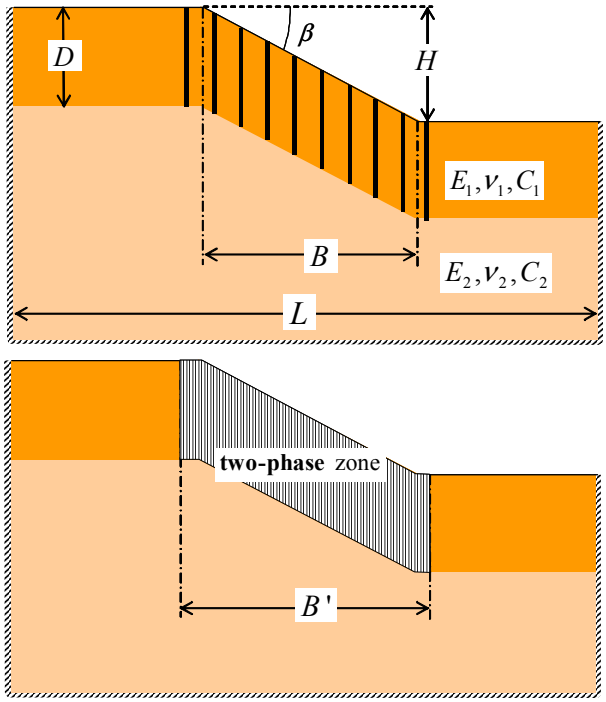

Figure 2. Stabilization of a slope by vertical inclusions

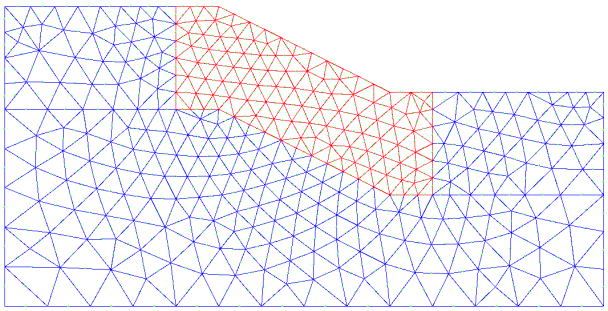

Figure 3 Finite element mesh used for the different simulations

A finite element mesh of the structure comprising 620 six-noded triangular elements and 1303 nodes has been adopted for the different simulations, as shown in Figure 3. The decisive advantage of the two-phase model is thus clearly apparent from this figure, since the direct implementation of the finite element method on the reinforced structure would have required a much more refined discretization of the structure in the reinforced zone, in order to capture the complex interactions prevailing between the soil and the dense network of cylindrical piles.

It should be emphasized in particular that the typical size of the mesh elements in the reinforced zone is in no way different from that adopted in the absence of reinforcement, and no remeshing procedure is required when the different characteristics of the reinforcements (spacing, diameter, thickness etc.) have to be changed.

The elastic as well as plastic parameters of the two-phase constituents to be introduced in the calculations, may then be determined as follows. It is first to be noted that, in the reinforced zone, the *reinforcement volume fraction* can be easily calculated as the ratio between the cross-sectional area of one individual pile and the total cross section s^2 of the representative volume of reinforced soil, namely:

$$\eta=\frac{2\pi Rt}{s^2}\cong 0.5\% \tag{30}$$

so that the soil volume fraction, equal to 1-η is close to unity. Therefore, it seems reasonable to adopt for the matrix phase in the reinforced zone, the same elastic and plastic characteristics as the corresponding upper soil layer, that is:

$$E^m\cong E_1=5\,\text{MPa}\,,\nu^m\cong\nu_1=0.3\,,\ C^m\cong C_1=5\,\text{kPa} \tag{31}$$

As regards the reinforcement phase, the axial, shear and bending stiffness densities are simply calculated, by dividing the corresponding quantities relative to one individual reinforcing inclusion by the area s^2 of the representative volume's cross section. One obtains from this straightforward procedure:

$$\begin{cases}\alpha^r=\dfrac{AE^s}{s^2}=1004\ \text{MPa}\\ \beta^r=\dfrac{A^*\mu^s}{s^2}=193\ \text{MPa}\\ \gamma^r=\dfrac{IE^s}{s^2}=502\ \text{MPa.m}^2\end{cases} \tag{32}$$

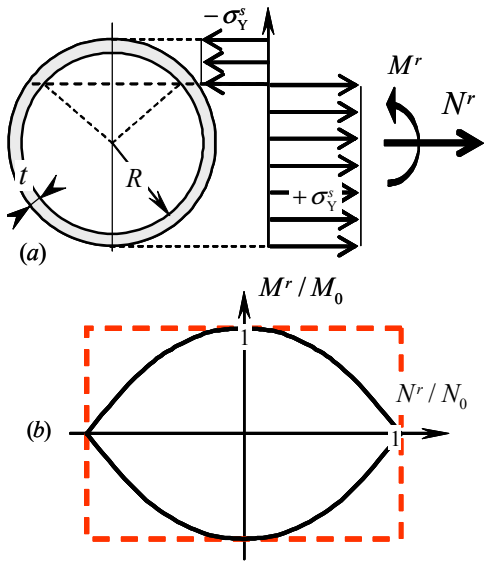

Figure 3 Interaction diagram for an individual reinforcing pile

where $A=2\pi Rt$ is the inclusion cross sectional area, $A^*=A/2$ its reduced cross sectional area (see for instance Frey, 1994), $I=\pi R^3 t$ its moment of inertia about its diameter and μ^s the steel shear modulus.

Likewise, the reinforcement phase yield strength properties, expressed by means of a criterion such as (8), may be determined from the solution to a yield design problem, sketched in Figure 3*a*, in which a section of pile is submitted to the combination of an axial force N^r and bending moment M^r. Exploring uniaxial stress distributions in the pile cross-section, as that sketched in Figure 4*a*, allows to derive the following interaction formula for a single pile (Challamel and de Buhan, 2003):

$$\left|\frac{M^r}{M_0}\right|-\cos\left(\frac{\pi}{2}\frac{N^r}{N_0}\right)\le 0\quad\text{with}\quad\begin{cases}N_0=2\pi Rt\,\sigma_Y^s\\ M_0=4R^2t\,\sigma_Y^s\end{cases} \tag{33}$$

This interaction formula, which is represented in Figure 3*b* (solid line), implicitly assumes that the pile is infinitely resistant to shear forces. It follows that the reinforcement phase yield strength condition (8) writes:

$$f^r(n^r,m^r)=\left|\frac{m^r}{m_0}\right|-\cos\left(\frac{\pi}{2}\frac{n^r}{n_0}\right)\le 0$$
$$\text{with}\begin{cases}n_0=2\pi Rt\,\sigma_Y^s/s^2=\eta\,\sigma_Y^s\cong 1\,\text{MPa}\\ m_0=4R^2t\,\sigma_Y^s/s^2=\dfrac{2}{\pi}\eta R\sigma_Y^s\cong 0.64\,\text{MPa.m}\end{cases} \tag{34}$$

which, for the sake of simplicity in the subsequent elastoplastic calculations, will be approximated by the following *upper bound* condition (dashed rectangle in Figure 3*b*):

$$\left|n^r/n_0\right|\le 1\ ,\ \left|m^r/m_0\right|\le 1 \tag{35}$$

7 RESULTS OF NUMERICAL SIMULATIONS

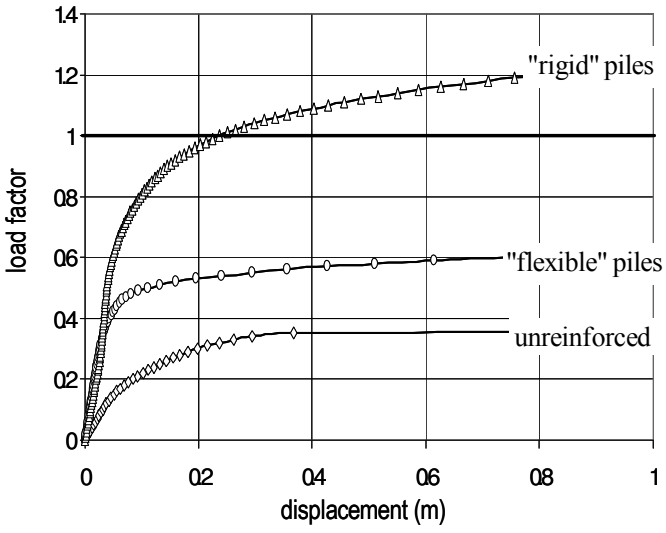

Figure 4. Simulated load-displacement curves for unreinforced and reinforced slope

First of all, a preliminary simulation is performed on the non reinforced structure. The result is shown in Figure 4 in

the form of a curve, drawn in the lower part of this figure, showing the evolution of an increasing proportion of the weight applied to the structure (load factor) as a function of the displacement of a point located at the top of the slope. It is clearly apparent that the prescribed weight loading by far exceeds the limit load of the unreinforced slope, which corresponds to a load factor equal to 0.35.

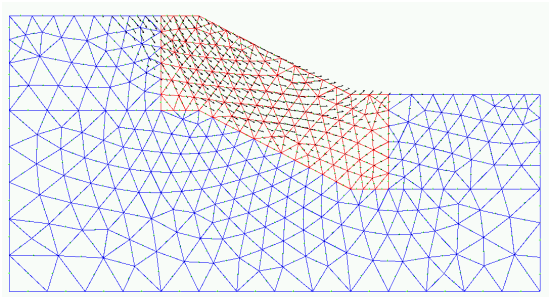

(*a*)

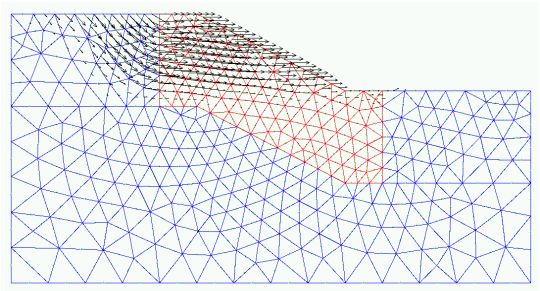

(*b*)

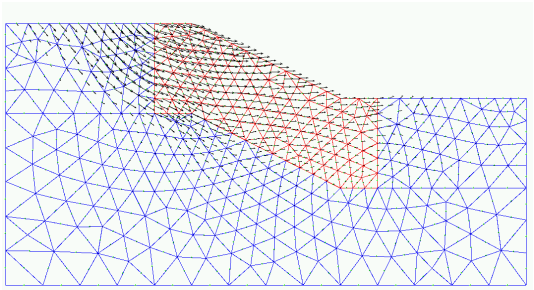

(*c*)

Figure 5 Failure mechanisms of (*a*) unreinforced slope and slope reinforced by (*b*) "flexible" or (c) "rigid" piles.

The middle curve corresponds to the simulation of the reinforced slope when shear and flexural effects of the reinforcements are neglected ($\beta^r=\gamma^r=0$, $m_0=0$), their stiffness and strength characteristics being held constant: case of "flexible" inclusions. Even though the limit load factor of the slope for which failure occurs is higher than that of the non reinforced structure, it still remains well below the prescribed weight loading (0.6<1).

Finally the upper curve is associated with the situation when the shear and flexural stiffness and strength capacities of the reinforcements are accounted for in the analysis. It clearly shows that the ultimate load is almost 25% higher than the prescribed loading, thereby ensuring the stabilization of the slope under its own weight.

Figure 5 pictures the failure mechanisms corresponding to the three above described elastoplastic simulations.

CONCLUDING REMARKS

The above results are fully consistent with those recently presented for piled raft foundations subjected to a combination of vertical and lateral loadings, associated with an overturning moment (Hassen and de Buhan, 2005*a* and *b*). They do confirm that the shear and flexural properties of the reinforcements play a decisive role in the global response of a reinforced slope. This has important consequences in terms of engineering design methods and optimization procedures applied to this kind of reinforced soil structures.

Indeed, as it has been pointed out in (Hassen and de Buhan, 2005*b*), the case when shear and flexural effects of the reinforcements could be discarded, actually corresponds to the situation when a large number of piles of small diameter is used instead of relatively few piles of large diameter, the volume fraction of reinforcing material given by Eq. (30), and thus the axial stiffness and strength properties of the reinforcement phase, being kept constant.

REFERENCES

de Buhan P., Sudret B. (2000). Micropolar multiphase model for materials reinforced by linear inclusions. *Eur. J. Mech. A/Solids* 19, p. 669-687

Challamel N., de Buhan P. (2003). Mixed modelling applied to soil-pipe interaction. *Comp. and Geotech*., 30, pp. 205-216.

Crisfield M.A. (1991). *Non-linear Finite Element Analysis of Solids and Structures*, *Vol.1: Essentials*. Wiley, New-York.

Frey F. (1994). *Analyse des structures et milieux continus*. Vol. 2, Presses Polytechniques et Universitaires Romandes

Hassen G., de Buhan P. (2005*a*). A two-phase model and related numerical tool for the design of soil structures reinforced by stiff linear inclusions. *Eur. J. Mech. A/Solids* 24, p. 987-1001

Hassen G., de Buhan P. (2005*b*) Elastoplastic multiphase model for simulating the response of piled raft foundations subject to combined loadings. *Accepted for publication in Int. J. Num. Anal. Meth. Geomech.*

Simo J.C., Hughes T.J.R. (1998). *Computational Inelasticity*. Springer, Berlin.

Sudret B. (1999). *Multiphase model for inclusion-reinforced structures*. PhD thesis, ENPC, Paris.